

BRCA1 Mutation Status and Follicular Fluid Exposure Alters NFκB Signaling and ISGylation in Human Fallopian Tube Epithelial Cells^{1,2}



Julia Hollingsworth^{*,†,‡,3}, Angela Lau^{*,‡,5,3},
Alicia Tone^{‡,#,3}, Alexandra Kollara^{*,‡}, Lisa Allen[‡],
Terence J. Colgan^{*,¶,**}, Valerie Dube^{¶,††,4},
Barry Rosen^{‡,#,5}, K. Joan Murphy^{‡,#,4},
Ellen M. Greenblatt^{*,‡}, Tomer Feigenberg^{‡,#,4},
Carl Virtanen^{††} and Theodore J. Brown^{*,†,‡,5}

*The Lunenfeld-Tanenbaum Research Institute of Mount Sinai Hospital, Toronto, ON; †Institute of Medical Sciences, University of Toronto, Toronto, ON; ‡Department of Obstetrics and Gynecology, University of Toronto, Toronto, ON; §Department of Physiology, University of Toronto, Toronto, ON; ¶Department of Laboratory Medicine and Pathobiology, University of Toronto, Toronto, ON; #Division of Gynecologic Oncology, Princess Margaret Cancer Centre, Toronto, ON; **Pathology and Laboratory Medicine, Mount Sinai Hospital, Toronto, ON; ††Department of Pathology, Women's College Hospital, Toronto, ON; ††Princess Margaret Genomics Centre, Toronto, ON

Abstract

Germline *BRCA1* or *BRCA2* mutations (mt*BRCA1* and mt*BRCA2*) increase risk for high-grade serous ovarian cancer (HGSOC), the most commonly diagnosed epithelial ovarian cancer histotype. Other identified risk factors for this cancer, which originates primarily in the distal fallopian tube epithelium (FTE), implicate ovulation, during which the FTE cells become transiently exposed to follicular fluid (FF). To test whether mt*BRCA1* or mt*BRCA2* nonmalignant FTE cells respond differently to periovulatory FF exposure than control patient FTE cells, gene expression profiles from primary FTE cultures derived from *BRCA1* or *BRCA2* mutation carriers or control patients were compared at baseline, 24 hours after FF exposure, and 24 hours after FF replacement with culture medium. Hierarchical clustering revealed both FF exposure and *BRCA* mutation status affect gene expression, with *BRCA1* mutation having the greatest impact. Gene set enrichment analysis revealed increased NFκB and EGFR signaling at baseline in mt*BRCA1* samples, with increased interferon target gene expression, including members of the ISGylation pathway, observed after recovery from FF exposure. Gene set enrichment analysis did not identify altered pathway signaling in mt*BRCA2* samples. An inverse relationship between EGFR signaling and ISGylation with *BRCA1* protein levels was verified in an immortalized FTE cell line, OE-E6/E7, stably transfected with *BRCA1* cDNA. Suppression of ISG15 and ISGylated protein levels by increased *BRCA1* expression was found to be mediated by decreased NFκB signaling.

Abbreviations: ACHP, 2-amino-6-[2-(cyclopropylmethoxy)-6-hydroxyphenyl]-4-(4-piperidinyl)-3-pyridinecarbonitrile; *BRCA1*, breast cancer 1, early onset; *BRCA2*, breast cancer 2, early onset; EGFR, epidermal growth factor receptor; FBS, fetal bovine serum; FDR, false discovery rate; FF, follicular fluid; FTE, fallopian tube epithelium; GO, Gene Ontology; GSEA, gene set enrichment analysis; HGSOC, high-grade serous ovarian cancer; mt*BRCA1*, *BRCA1* mutation; mt*BRCA2*, *BRCA2* mutation.

Address all correspondence to: Theodore J. Brown, PhD, Lunenfeld-Tanenbaum Research Institute at Mt. Sinai Hospital, 60 Murray Street, Box 42, Toronto, ON M5T 3L9.

E-mail: brown@lunenfeld.ca

¹Funding: This work was supported by the Canadian Institute of Health Research (grant number MOP106679, 2017). J. H. was supported by a Kristi Piia Callum Memorial Fellowship in Ovarian Cancer.

²Declarations of Interest: None.

³Contributed equally to the work.

⁴Present affiliation: Trillium Health Partners; Mississauga, ON, Canada.

⁵Present affiliation: Beaumont Health System; Royal Oak, MI, USA.

Received 13 April 2018; Revised 7 May 2018; Accepted 11 May 2018

© 2018 The Authors. Published by Elsevier Inc. on behalf of Neoplasia Press, Inc. This is an open access article under the CC BY-NC-ND license (<http://creativecommons.org/licenses/by-nc-nd/4.0/>).

<https://doi.org/10.1016/j.j.neo.2018.05.005>

These studies indicate that increased NF κ B signaling associated with decreased BRCA1 expression results in increased ISG15 and protein ISGylation following FF exposure, which may be involved in predisposition to HGSOc.

Neoplasia (2018) 20, 697–709

Introduction

Ovarian cancers of epithelial derivation are composed of multiple histotypes that differ in commonly mutated genes, clinical course, and presumed cell of origin. Among these histotypes, high-grade serous ovarian cancer (HGSOc), which originates primarily in the fimbrial fallopian tube epithelium (FTE), accounts for the majority of deaths [1]. The most significant risk factor for HGSOc is a family history of breast or ovarian cancer, with heritable mutations in *breast cancer 1, early onset (BRCA1)* or *breast cancer 2, early onset (BRCA2)* genes conferring most of this familial risk. Germline *BRCA1* mutation (mt*BRCA1*) carriers have a lifetime HGSOc risk of up to 60% compared to 1.4% to 1.7% for the general female population, whereas germline *BRCA2* mutation (mt*BRCA2*) carriers have a lifetime risk of up to 23% [2–4]. mt*BRCA1* carriers also tend to be diagnosed at an earlier age than either mt*BRCA2* carriers or sporadic cases [5], suggesting acceleration of the carcinogenic process by *BRCA1* insufficiency.

Additional risk factors for HGSOc are consistent with a promoting role for an increased number of lifetime ovulatory events. The use of oral contraceptives, increased parity, lactation, early menopause, and potentially late menarche reduce risk in the general population [6,7] and in mt*BRCA1* and mt*BRCA2* carriers [8,9]. Ovulation is a recurring event involving a cascade of inflammatory signaling pathways triggered by the LH surge that culminates in the release of the cumulus-oocyte complex and follicular fluid (FF) into the fimbria of the fallopian tube. As a result of the dynamic intrafollicular signaling leading up to ovulation, this periovulatory FF contains cytokines, chemokines, free radicals, and steroid hormones [10]. Repetitive exposure of the FTE to these FF factors could promote carcinogenesis, perhaps through increased DNA adduct formation and gene mutation to drive development of HGSOc precursors in the distal FTE [11].

We previously reported that gene expression profiles from nonmalignant FTE from mt*BRCA1* carriers obtained during the postovulatory luteal phase more closely resembled HGSOc than FTE either from control patients or from mt*BRCA1* carriers obtained during the follicular phase [12]. Further characterization of the molecular differences indicated an increased expression of proinflammatory genes in luteal phase FTE from mt*BRCA1* carriers [13]. This surprising finding suggested that FTE from mt*BRCA1* carriers might respond differently to ovulation or to the luteal phase milieu.

The primary objective of the current study was to determine whether the response to FF exposure of nonmalignant FTE cells derived from mt*BRCA1* or mt*BRCA2* carriers differs from that of cells derived from control patients. Our findings demonstrate increased inflammatory and epidermal growth factor receptor (EGFR) pathway signaling in FTE from *BRCA1* mutation carriers. We also provide evidence of increased ISGylation, a posttranslational protein modification, in *BRCA1*-deficient cells following exposure to

periovulatory FF, raising the possibility that this pathway may contribute to predisposition to HGSOc.

Materials and Methods

Patient Samples

Fallopian tube surgical specimens were obtained from 24 women with either known *BRCA1* mutations ($n=8$) or known *BRCA2* mutations ($n=8$), or with no personal or known family history of breast or ovarian cancer ($n=8$). All mt*BRCA1* and mt*BRCA2* carriers underwent risk-reducing salpingo-oophorectomy, whereas control patients underwent surgery for benign conditions (Table 1). The study was approved by Mount Sinai Hospital and Women's College Hospital Research Ethics Boards, and all patients provided informed consent prior to tissue donation.

Primary FTE Culture

Tissue fragments were washed, minced, and incubated for 48 hours in MEM (Invitrogen, Burlington, Canada) containing 1.4 mg/ml Pronase and 0.1 mg/ml DNase I (Roche Diagnostics, Laval, Canada)

Table 1. Age and *BRCA1* and *BRCA2* Mutations for Patients Contributing Surgical Samples for FTE Derivation a

Patient ID	Age (Years)	Indication for Surgery	Mutation Status
BRCA1			
1	50	RRSO	c.5266dupC
2	38	RRSO	5083del19
3	49	RRSO	c.4484G>T
4	38	RRSO	3875delGTCT
5	38	RRSO	c.1994delA
6	41	RRSO	c.4484G>T
7	39	RRSO	5382insC
8	41	RRSO	185delAG
BRCA2			
9	37	RRSO	3331G>T
10	44	RRSO	6884C>G
11	33	RRSO	5972C>T
12	48	RRSO	c.9435_9436delGT
13	51	RRSO	c.517-2A>G
14	54	RRSO	3036delACAA
15	41	RRSO	c.5909C>A
16	42	RRSO	9894delT
Control			
17	56	Uterine fibroids	N/D
18	52	Uterine fibroids	N/D
19	54	Endometrial hyperplasia	N/D
20	50	Dermatoid cyst	N/D
21	33	Uterine fibroids	N/D
22	52	Uterine fibroids	N/D
23	48	Uterine fibroids	N/D
24	47	Uterine fibroids	N/D

RRSO, risk-reducing salpingo-oophorectomy; N/D, not determined.

^a The average age (\pm SEM) for *BRCA1* mutation carriers, *BRCA2* mutation carriers, and control patients was 41.7 (\pm 1.7), 43.7 (\pm 2.5), and 49.0 (\pm 2.5) years, respectively [$F_{(2, 21)}=2.698$, $P=.091$].

at 4°C. Enzymes were inactivated by addition of fetal bovine serum (FBS) to 10% (v/v). Dissociated cells were collected; resuspended in DMEM supplemented with 10% FBS, 100 U/ml penicillin, 100 µg/ml streptomycin, and 0.625 µg amphotericin (Invitrogen); and transferred to a positively charged culture plate for 3 to 4 hours. Nonadherent cells were collected and seeded onto collagen type IV-coated Transwell inserts at >75% confluency, as previously described [14]. All cultures were maintained with culture medium in both chambers. Medium was replaced every 48 hours until cultures were confluent. Cultures consisted of 49.6%±2.9% (mean±SEM) secretory epithelial cells, 38.0%±2.0% ciliated epithelial cells, and 11.7%±1.6% stromal cells, as determined by immunostaining for Pax8 (ProteinTech, Rosemont, IL), FoxJ1 (Abcam, Cambridge, MA), and vimentin (Dako, Mississauga, Canada), respectively ($n=4$).

OE-E6/E7 Cell Culture

OE-E6/E7 cells [15], obtained from Dr. William S. B. Yeung, University of Hong Kong (China), were maintained in DMEM supplemented with 10% FBS, 100 U/ml penicillin, and 100 mg/ml streptomycin. Short tandem repeat analysis performed for 10 markers verified a human female derivation, and all experiments were conducted within 10 passages from the starting stock culture. A PCR detection kit (Applied Biological Materials Inc., Richmond, BC) was used to test for mycoplasma.

OE-BRCA1 cells were generated by stable transfection with a wild-type *BRCA1* expression construct generated by ligating *BRCA1* cDNA from pcBRCA1-385 (Addgene, Cambridge, MA) into pcDNA3.1H⁺ (Invitrogen). OE-Mock cells were transfected in parallel with empty pcDNA3.1H⁺. Stable transfectants were selected using 80 µg/ml Hygromycin B (Invitrogen).

2-Amino-6-[2-(cyclopropylmethoxy)-6-hydroxyphenyl]-4-(4-piperidinyl)-3-pyridinecarbonitrile (ACHP) (Tocris, Minneapolis, MN) was dissolved in DMSO. Cells were treated with 1 to 25 µM in culture medium for 48 hours. Recombinant human IFN-β (R&D, Minneapolis, MN) was reconstituted in water. Cells were treated with 1000 U/ml culture medium.

Ovarian Cancer Cell Lines

SKOV3, ES-2, and HEY ovarian cancer cell lines were grown in RPMI-1640 culture medium supplemented with 5% FBS, 100 U/ml penicillin, and 100 mg/ml streptomycin. UWB1.289 and UWB1.289 +BRCA1 ovarian cancer cells were grown in a 1:1 ratio of RPMI-1640 with mammary epithelial growth medium (ATCC, Manassas, VA). Medium for UWB1.289 +BRCA1 was further supplemented with G418. All cell lines were verified by STR analysis and tested for mycoplasma as described.

Periovarulatory FF Treatment

FF was obtained from the leading follicle from 14 consenting patients undergoing oocyte retrieval as part of their *in vitro* fertilization treatment at Mount Sinai Hospital Fertility Center. The FF samples were subjected to cytokine profiling, which was previously reported [16], and was pooled and stored at -80°C. Once FTE cultures reached confluency (2-3 weeks), culture medium in the upper Transwell chamber was replaced with 100 µl filter-sterilized FF for 24 hours followed by replacement with fresh culture medium. Paired baseline cultures were treated in parallel, except culture medium was used instead of FF. The lower chamber contained culture medium alone for all cultures.

See Figure 1 for treatment schematic. Exposure of FTE cells to undiluted FF increases rather than decreases cell number [17] (Supplementary Figure S1), indicating that this treatment was not toxic to cells.

Gene Expression Profiling and Analysis

RNA was extracted from primary FTE cultures using TRIzol (Invitrogen), further purified using an RNeasy MiniElute cleanup kit (Qiagen, Toronto, Canada), and quantified by NanoDrop spectrophotometry. All samples had a minimum RNA integrity value of 8.0 (Agilent bioanalyzer system). Whole genome transcriptome profiling was performed at the Princess Margaret Genomics Centre. RNA (200 ng) was labeled using Illumina TotalPrep-96 RNA amplification kit (Thermo Fisher Scientific, Burlington, Canada), and 750 ng of resulting cDNA was hybridized onto Illumina Human HT-12 v4.0 Beadchip Arrays. The beadchips were washed and stained per Illumina protocol and scanned on an iScan (Illumina) scanner. Gene expression profiling data are available at NCBI Gene Expression Omnibus (GEO; <http://www.ncbi.nlm.nih.gov/geo>, accession number GSE98699).

Microarray data were converted to log₂ and quantile median-normalized using Genespring v12.1 software. Samples were run in two balanced batches due to the interval in collecting patient derived material; therefore, a further batch effect normalization was performed using CombatR [18]. Unsupervised hierarchical clustering using average linkage rules and Pearson-centered metrics was performed to assess the overall degree of gene expression similarity among samples. All probes were filtered prior to analysis to remove probes showing no signal across all three sample groups (80% of samples in either group having expression in the 20th to 100th percentile of measured signal values). A one-way ANOVA with a TUKEY HSD using Benjamini-Hochberg false discovery rate (FDR) for each comparison was used to identify probes whose mean expression was different between genotypes at each time point.

Gene Ontology (GO) analysis was performed on genes significantly different with a 1.5-fold change cutoff between mt*BRCA1* or mt*BRCA2* and control samples at the three time points using an FDR <0.3. GSEA was performed between patient groups at the three time points using GSEA software version 2.2.2 and predefined gene sets from the Molecular Signatures Database (MSigDB v5.0). Analysis between patient groups at the three time points involved 1000 permutations using the signal2noise metric. Gene sets with an FDR <0.25 were identified and interactions between gene sets were visualized with Cytoscape software [19].

Quantitative Real-Time RT-PCR (RT-qPCR)

RNA was extracted from OE-E6/E7 cells with an RNeasy Plus Universal Mini Kit (Qiagen), and transcript levels for *IL8*, *TNF*, *HRAS*, *ISG15*, *HERC5*, *USP18* in OE-Mock and OE-BRCA1 cells were measured by RT-qPCR using primers shown in Supplementary Table S1. RNA was reverse transcribed using Superscript III and random hexamers (Invitrogen). qPCR was performed using an ABI PRISM 7900HT sequence detection system (Invitrogen) with SYBR Green PCR Master Mix (Invitrogen) and analyzed using the ΔCCT method. Target gene C_T were normalized to the geometric mean of three housekeeping genes, *GAPDH*, *YWHAZ*, and *B2M*, using standard curves. Data are expressed as mean±SEM.

Western Blot Analysis

Cellular proteins were extracted using RIPA lysis buffer (50 mM HEPES, 150 mM NaCl, 1% Triton X-100, 0.1% SDS, 1% sodium deoxycholate) containing protease and phosphatase inhibitors (Roche Diagnostics) and quantified using BCA Protein Assay Kit (Thermo Fisher Scientific). Protein extracts were resolved by SDS-PAGE, transferred to PVDF membranes, and immunoblotted with anti-BRCA1 (1:500; sc-6954, Santa Cruz Biotechnology, Dallas, TX), anti-ISG15 (1:2000, a gift from Dr. Arthur Haas, Louisiana State University) [20], anti-EGFR (1:1000, #2232), anti-pERK1/2 (1:2000, #9101), anti-ERK1/2 (1:2000, #4696), anti-USP18 (1:1000, #4813) (Cell Signaling Technology, Danvers, MA), anti-tubulin (1:3000, #T6199, Sigma), or anti-HSP90 (1:5000, #610418, BD Transduction Laboratories, Mississauga, Canada) antibodies. Immunoblots were then incubated with horseradish peroxidase-conjugated goat anti-rabbit (1:1000, sc-2004, Santa Cruz Biotechnology) or horse anti-mouse antibodies (1:1000, #7076, Cell Signaling Technology). Immunoreactive bands were visualized by enhanced chemiluminescence (Santa Cruz Biotechnology) and quantified using ImageJ software.

Statistical Analysis

RT-qPCR and Western blot data were analyzed by one-sample *t* test, one-way ANOVA followed by a Student-Neuman-Keuls (SNK) *post hoc* test, or two-way ANOVA (Prism 5). Comparisons were considered statistically significant at $P < .05$.

Results

mtBRCA Status and FF Exposure Alter Gene Expression Profiles

Primary FTE cell cultures derived from mtBRCA1 or mtBRCA2 carriers or control patients were grown on collagen IV-coated tissue culture Transwells to simulate *in vivo* FTE structure [14]. Periovarian human FF was added to the upper chamber for 24 hours to simulate transient apical FTE ovulatory exposure *in vivo*. Genome-wide gene expression profiles were obtained 24 hours after FF addition ($t = F24$, acute response) and 24 hours after its replacement with culture medium ($t = FC$, recovery). Paired baseline ($t = C24$ and C48) cultures were treated in parallel, except that culture medium was used instead of FF (Figure 1). Since analysis indicated no differences in gene expression between baseline cultures collected at 24 and 48 hours, only baseline data obtained at 24 hours (C24) were included in further analysis.

Unsupervised hierarchical clustering of all 72 culture samples (24 patients \times 3 time points) based upon overall gene expression resulted in all three time point samples (C24, F24, FC) from each patient clustering most closely together for 20 of the 24 patients (Figure 2A). While this pattern largely reflects patient variation, an impact of mtBRCA status was indicated. The 72 samples partitioned into 3 main clusters, with mtBRCA1 samples dominating one cluster (Group 1A; 67% of mtBRCA1, 33% of mtBRCA2, and 4% control). A second and smaller cluster (Group 1B) contained no mtBRCA1, 25% of mtBRCA2, and 12.5% of control patient samples, whereas the third and largest cluster was dominated by control patient samples (Group 2; 83% of control, 33% of mtBRCA1, and 42% of mtBRCA2). Samples did not partition based upon FF exposure, indicating that mtBRCA status had a greater impact on overall gene expression than FF.

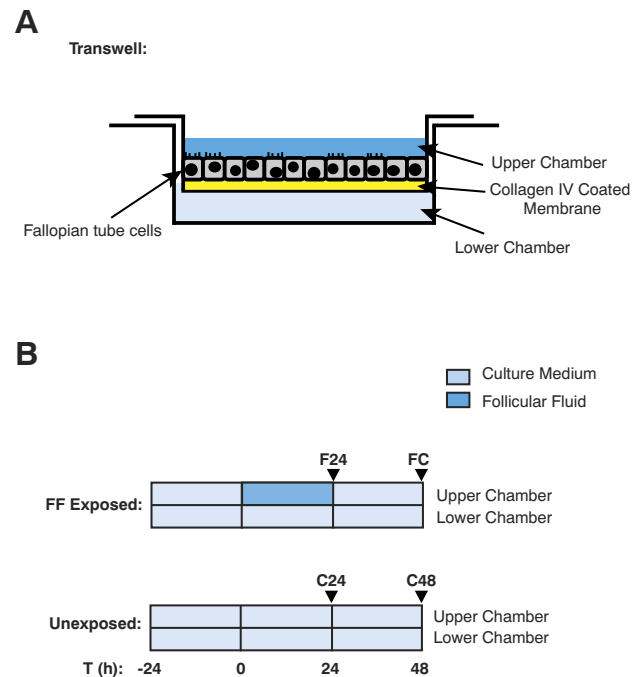


Figure 1. Schematic showing the treatment paradigm. Dissociated fallopian tube epithelial cells were seeded into the upper chamber of 24-well Transwells coated with collagen IV and grown to confluence (A). Follicular fluid (FF) was added to the upper chamber and was replaced with culture medium after 24 hours (B). Cells were harvested 24 hours after FF addition (F24) or 24 hours after replacing FF with culture medium (FC). Parallel cultures from each patient were treated similarly except that culture medium was used instead of FF (C24 and C48).

One-way analysis of variance identified 4218 probesets with differential expression between all 9 groups (3 genotypes \times 3 timepoints). Clustering of samples based upon these genes revealed three principal groupings, with mtBRCA1 samples largely partitioning separately (Group 1) from control patient samples (Group 2B), and mtBRCA2 samples distributed evenly within the groupings (Figure 2B). While this pattern further indicates that mutation status has the greatest impact on gene expression, an impact of FF exposure was also evident, as 83% of F24 samples partitioned away from their matched baseline sample. Moreover, a subgroup of F24 samples from all three patient categories clustered together in Group 2A (3 control, 4 mtBRCA1, 5 mtBRCA2).

Differentially Expressed Genes Based Upon mtBRCA Status Are Affected by FF Exposure

The overlap in genes differentially expressed based on mtBRCA status at baseline (C24) and after FF exposure (F24 and FC) is shown in Figure 3. A greater number of probesets were differentially expressed between mtBRCA1 versus control patient samples at all time points, as compared to mtBRCA2 versus controls. At baseline, 831 probesets were differentially expressed in mtBRCA1 samples, and 460 probesets were differentially expressed in mtBRCA2 samples, as compared to control patient samples. With acute FF exposure (F24), the number of differentially expressed probesets decreased (615 for mtBRCA1 and 111 for mtBRCA2), and this number increased upon recovery from FF exposure (FC) to 1198 for mtBRCA1 and 337 for mtBRCA2. Approximately half of the genes differentially expressed in

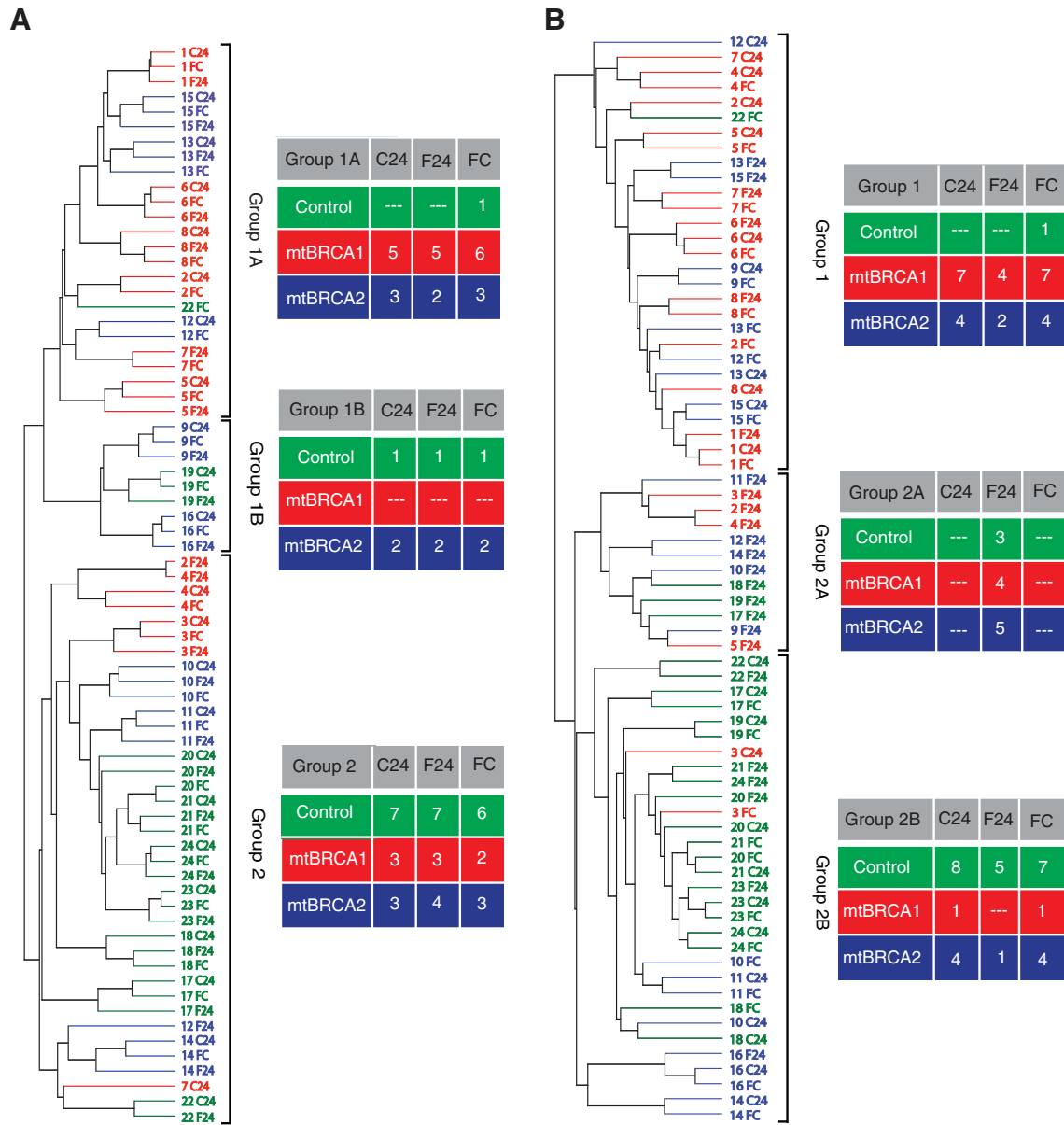


Figure 2. Hierarchical clustering of FTE samples based on gene expression profiles indicates an impact of BRCA1 and BRCA2 mutation status and FF exposure. (A) Dendrogram resulting from unsupervised hierarchical clustering of all culture samples based upon expression of all filtered gene probesets. (B) Hierarchical clustering of all culture samples based upon expression of 4218 gene probesets identified as significantly different by one-way ANOVA. *mtBRCA1* samples are coded in red, *mtBRCA2* samples are coded in blue, and control patient culture samples are coded in green. Sample identification numbers correspond to patient numbers shown in Table 1.

mtBRCA2 samples versus control patient samples were also differentially expressed in *mtBRCA1* samples versus control patient samples (Figure 3).

At FC, there were 44% more probesets differentially expressed between *mtBRCA1* and control patients than at baseline (1198 vs 831) (Figure 3), whereas the number of differentially expressed genes in *mtBRCA2* samples was decreased by 27% (337 vs 460). Moreover, no more than 50% of gene probesets identified as differentially expressed at FC overlapped with either C24 or F24 for *mtBRCA1* or *mtBRCA2* samples (Supplementary Figure S2). This suggests a delayed differential response to FF exposure based on *mtBRCA* status.

mtBRCA1 Status Impacts Immune and EGFR Signaling Pathway-Associated Genes

To derive a functional profile of differentially expressed genes at each time point, GO analyses were performed on genes significantly different with a 1.5-fold change cutoff between *mtBRCA1* or *mtBRCA2* and control samples. At baseline, genes increased and decreased in *mtBRCA1* samples associated with 17 and 20 GO terms, respectively (Supplementary Table S2). No GO terms associated with genes increased at F24 in *mtBRCA1*, whereas 7 GO terms associated with decreased genes. At FC, 7 GO terms associated with genes increased in *mtBRCA1*, and 21 GO terms associated with decreased genes.

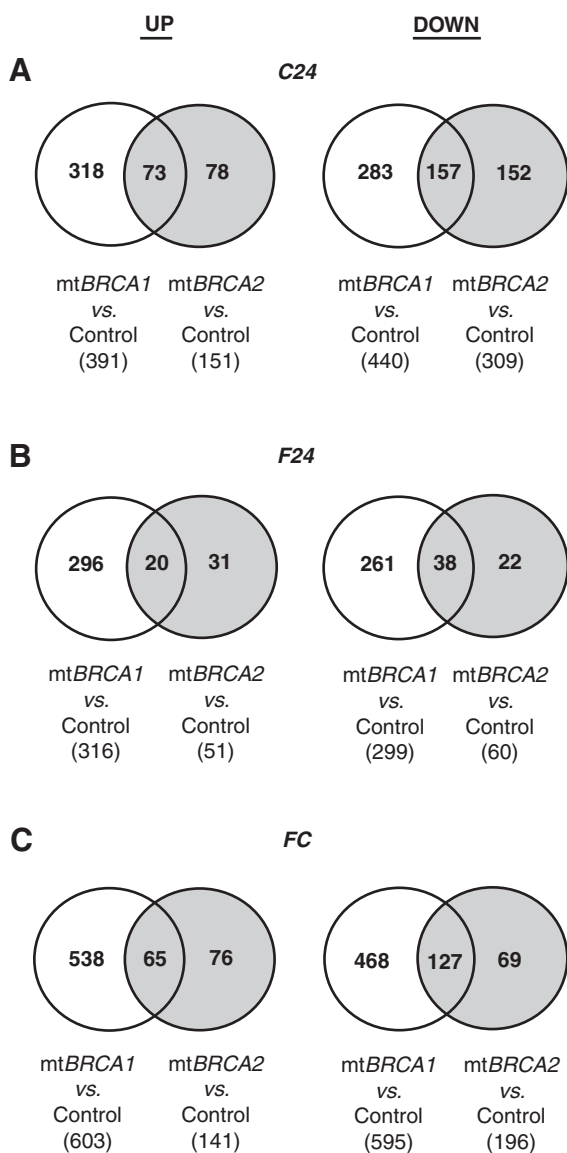


Figure 3. *mtBRCA1* samples have a greater number of significantly different genes than *mtBRCA2* samples relative to control FTE at all time points. Overlap of statistically significant differentially expressed gene probesets in *mtBRCA1* and *mtBRCA2* samples relative to control patient samples is shown (A) at baseline (C24), (B) after 24 hours of FF exposure (F24), and (C) after 24 hours of recovery following FF exposure (FC). Numbers provided are the number of probesets significantly different based upon one-way ANOVA ($P < .05$). The number of genes with increased expression in BRCA mutants versus control is in the left column, and that with decreased expression in BRCA mutants versus control is in the right column.

GO terms identified at all three time points were primarily associated with inflammation and immune system: altogether, 61.4% (27 of 44) of the significant GO terms for *mtBRCA1* samples were related to the immune system. This suggests that most gene expression changes due to *mtBRCA1* status alone and to FF exposure involve alterations in immune response or cytokine signaling. Additionally, GO terms relating to proliferation, apoptosis, and cell-cell junction were associated with genes increased in *mtBRCA1* at baseline. New GO terms emerging at FC included response to virus, innate immune response, and activation of immune response

(Supplementary Table S2). In contrast, no GO terms associated with *mtBRCA2* differentially expressed genes either at baseline or FC. At F24, five GO terms were associated with decreased genes in *mtBRCA2* samples that were related to immune system response and function (Supplementary Table S3).

As opposed to GO analysis, GSEA is a multivariate tool that takes into account all changes in gene expression to identify multiple pathway members that collectively could amount to a larger impact on particular cell functions. GSEA was performed between all *mtBRCA* status groups at baseline, F24, and FC. Only comparisons between *mtBRCA1* versus control patients provided genesets with an FDR < 0.25 . A total of 246 genesets were upregulated in *mtBRCA1* versus control at baseline, while no genesets attained significance as downregulated. Many of these upregulated genesets are involved in inflammation, DNA damage, and growth pathways (Supplementary Table S4). Visualization of enriched geneset networks using Cytoscape revealed two large clusters: NF κ B-related and EGFR-related pathways (Figure 4A). At F24, the only geneset with an FDR < 0.25 for *mtBRCA1* versus control was “Reactome pyruvate metabolism,” which was decreased in *mtBRCA1* samples.

At FC, 182 genesets were associated with upregulated genes in *mtBRCA1* relative to control patient samples (Supplementary Table S5). Visualization revealed a large cluster of linked genesets involved with interferon signaling (Figure 4B). Genes forming the leading-edge subset within genesets represent those that contribute most to the enrichment score and have the largest fold-change in expression. The leading-edge gene subset of the top 20 genesets between *mtBRCA1* and control at FC, based upon the normalized enrichment score, is shown in Table 2. Among these, *ISG15* and some of its key interacting partners involved in ISGylation (*HERC5*, *HERC6* and *USP18*) were upregulated in *mtBRCA1* versus control samples. In fact, *ISG15* expression was 4.5-fold higher in *mtBRCA1* versus control samples and appears in 14 of the top 20 genesets at FC. Moreover, *ISG15* was upregulated 3.4-fold at baseline in *mtBRCA1* versus control samples.

Altering BRCA1 Levels Replicates Key Differences in Gene Expression

OE-E6/E7 immortalized human FTE cells were used to address whether changes in gene expression reflect BRCA1 levels as opposed to differential programming of the primary FTE cells *in vivo*. OE-E6/E7 cells express low levels of BRCA1 relative to HEY, ES2, and SKOV3 ovarian cancer cell lines (Figure 5A). Therefore, OE-E6/E7 cells were stably transfected with wild-type *BRCA1* (OE-BRCA1) or transfected with empty expression vector (OE-Mock), resulting in cells expressing high and low BRCA1 levels, respectively (Figure 5A). *TNF α* , *IL8*, *ISG15*, and *HRAS* were found to have increased expression in *mtBRCA1* samples at baseline and were selected for investigation. Consistent with our primary FTE gene expression profiles, *TNF α* , *IL8*, and *ISG15* transcript levels were suppressed by increased BRCA1 levels in OE-E6/E7 cells (Figure 5, B-D), whereas increased BRCA1 did not alter *HRAS* transcript levels (Figure 5E).

GSEA also indicated that FF treatment of primary FTE cultures transiently suppressed interferon-induced gene expression that was otherwise elevated in *mtBRCA1* samples at other time points. These genes included multiple regulators of the ISG15 protein modification pathway, including *HERC5* and *USP18*. To determine whether these differences could be due to differential BRCA1 levels, OE-Mock and OE-BRCA1 cells were treated with FF in a manner identical to the

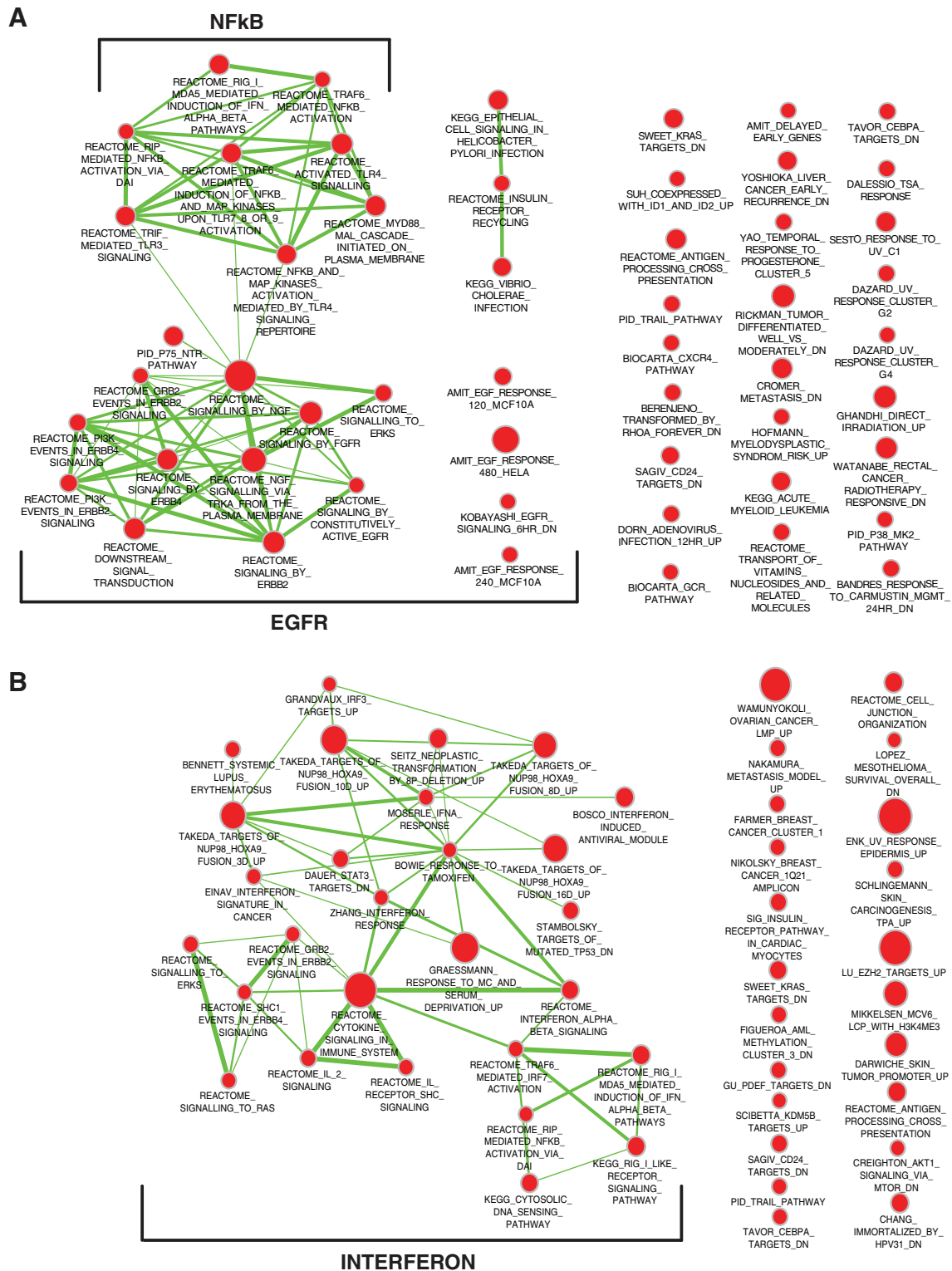


Figure 4. GSEA of gene expression profiles from *mtBRCA1* samples compared to control patient samples reveals three major gene clusters. (A) Cytoscape visualization of gene networks increased in *mtBRCA1* samples versus control patient samples at baseline (C24) showing two main clusters indicating altered NFkB and EGFR signaling. (B) Cytoscape visualization of gene networks increased in *mtBRCA1* samples versus control patient samples after 24 hours of recovery from FF exposure (FC) showing one main cluster of significant gene sets in *mtBRCA1*, which reflect altered interferon responsive genes. The size of the node reflects the number of genes within the geneset. Red nodes represent increased expression of the genes within the geneset in *mtBRCA1* versus control. Edge thickness reflects the number of genes that overlap between connected genesets. All GSEAs were performed using an FDR <0.25.

Table 2. Significantly Upregulated Genes from the Leading Edge Subset of the Top 20 Gene Sets from the GSEA Comparing mtBRCA1 and Control after Recovery from Follicular Fluid Exposure (FC)

Gene Symbol	Fold Change	# of Gene Sets Within Top 20	Gene Symbol	Fold Change	# of Gene Sets Within Top 20
IFIT1	6.38	13	FAM46A	1.86	1
OAS2	4.95	10	USP18	1.84	4
ISG15	4.50	14	PLAUR	1.80	1
IFIT3	3.69	12	SP110	1.78	5
MX1	3.62	13	IFIH1	1.78	6
CXCL10	3.41	5	DDX58	1.77	7
IFI44L	3.30	7	ITGB8	1.75	1
IRF7	3.10	12	DDX60	1.69	7
MX2	2.98	7	PAFAH1B3	1.63	1
RSAD2	2.97	5	EIF2AK2	1.62	5
OAS3	2.95	8	PARP12	1.61	5
OAS1	2.91	10	TSPAN1	1.60	1
IFI44	2.90	8	TAP1	1.58	2
HERC6	2.83	6	LAMP3	1.54	3
EPSTI1	2.78	3	ARTN	1.48	1
HS3ST1	2.72	1	PARP14	1.46	2
HERC5	2.35	6	ATP6V1F	1.45	1
OASL	2.29	10	YWHAB	1.45	3
HLA-C	2.29	1	PARP10	1.44	1
SAMD9L	2.27	3	CMPK2	1.43	3
IFIT2	2.26	5	IRF3	1.37	3
IFI35	2.21	11	ZBP1	1.33	4
XAF1	2.15	8	IFIT5	1.30	4
PRIC285	2.10	2	RIPK3	1.30	1
PARP9	2.07	3	DHX58	1.29	3
STAT1	2.06	9	NAGK	1.28	1
DDX60L	1.98	1	RTEL1	1.26	1
SAMD9	1.96	5	HRAS	1.11	1

primary FTE cultures. At baseline and FC, levels of *ISG15*, *HERC5*, and *USP18* transcripts were significantly greater in OE-Mock compared to OE-BRCA1 cells (Figure 5, F-H), indicating that high levels of BRCA1 suppress their expression. Treatment of OE-Mock cells with FF (F24) suppressed levels of all three transcripts to those measured in OE-BRCA1 cells at baseline.

The impact of BRCA1 expression on USP18 and conjugated and free ISG15 protein levels in OE-E6/E7 cells was investigated. Since expression of these genes is activated by type I interferon, protein levels were examined 24 hours after IFN β or vehicle treatment. In vehicle-treated cells, increased BRCA1 decreased both free ISG15 (Figure 6, A and B) and USP18 (Figure 6, D and E), which is consistent with our findings on transcript levels. As expected, similar levels of both proteins in OE-Mock and OE-BRCA1 cells were measured after IFN β treatment (Figure 6, B and F). Conjugated ISG15 levels were also increased in OE-Mock relative to OE-BRCA1 cells, and this difference persisted with IFN β treatment (Figure 6C).

Although EGFR mRNA was not increased in mtBRCA1 primary FTE cultures, GSEA indicated upregulation of EGFR signaling associated with lower levels of functional BRCA1. Consistent with this inverse relationship, increased BRCA1 expression in OE-E6/E7 cells decreased EGFR protein levels (Figure 6G and H).

Increased NF κ B Signaling in Cells with Low BRCA1 Levels Increases ISG15, EGFR, and pERK1/2

To investigate whether elevations in ISG15 and EGFR due to decreased BRCA1 levels are mediated through NF κ B signaling, OE-Mock and OE-BRCA1 cells were treated with increasing doses of the IKK α/β inhibitor ACHP. Consistent with our findings above, free and conjugated ISG15 (Figure 7, A-C) and EGFR (Figure 7, D and

E) levels were increased in OE-Mock cells relative to OE-BRCA1 cells. pERK1/2 levels, a downstream EGFR mediator, were also increased in OE-Mock cells (Figure 7, F-H). ACHP treatment decreased both free and conjugated ISG15 in OE-Mock cells to levels comparable to those in vehicle-treated OE-BRCA1 cells, whereas ACHP treatment did not alter ISG15 levels in OE-BRCA1 cells. Similarly, high (10 and 25 μ M) ACHP decreased EGFR protein levels in OE-Mock but not OE-BRCA1 cells. In contrast, pERK1/2 levels were reduced at high doses of ACHP similarly in both OE-Mock and OE-BRCA1 cells. This suggests that elevated ISG15, EGFR, and ERK1/2 activation levels observed in low BRCA1-expressing cells are due to increased NF κ B signaling.

Discussion

This study demonstrates that FTE cells from mtBRCA1 carriers have a gene expression profile that is distinct from that of FTE from control patients. Even in the absence of FF exposure, mtBRCA1 samples displayed molecular profiles indicative of increased inflammatory and EGFR signaling. Moreover, following recovery from FF exposure, an increased expression of type I interferon-responsive genes, including multiple members of the ISGylation protein modification pathway, was apparent in mtBRCA1 samples.

Numerous genes were also differentially expressed in mtBRCA2 samples compared to control patient samples. However, GSEA failed to identify statistically significant genesets. It is interesting to note that the top ranking genesets in mtBRCA2 versus control samples were similar to those significantly elevated in mtBRCA1 versus control samples, particularly after recovery from FF exposure. These were characterized by elevated interferon target genes (Supplementary Tables S6 and S7). Previous studies have shown increased interferon target gene expression in BRCA2-null colorectal carcinoma cells [21] and that BRCA2 binds the transcriptional repressor EMSY to suppress interferon gene expression [22]. Further studies are required to investigate the impact of BRCA2 mutations on interferon target gene expression and inflammatory signaling.

Chronic inflammatory signaling, which is mediated by NF κ B, is associated with precipitating events in carcinogenesis and is activated in nearly all cancers [23]. Key NF κ B target genes, including *TNF α* , *IL8*, and *ISG15*, were increased in mtBRCA1 FTE compared to that derived from control patients. Expression of BRCA1 in OE-E6/E7 cells decreased the levels of these transcripts, indicating that this is a direct result of decreased functional BRCA1. TNF α and IL8 promote leukocyte recruitment, and TNF α is a potent activator of further NF κ B signaling. Thus, increased expression of these cytokines would likely increase local inflammatory signaling *in vivo*. An increase in IL8 expression following FF exposure in non-BRCA1-deficient bovine and human oviductal cells was shown by us and others [16,17]. Notably, BRCA1-mutated luteal phase FTE grouping with HGSOc in our previous study showed increased *IL8* expression, in addition to other monocyte/neutrophil chemokines [12].

We previously demonstrated that decreasing BRCA1 expression in ES2 ovarian and A549 lung cancer cells enhanced NF κ B signaling [13], but the precise mechanism involved is not clear. Sau et al. [24] similarly found increased NF κ B signaling in BRCA1-deficient mammary gland progenitor cells, which they attributed to the DNA damage response. However, BRCA1 binds RelA/p65 and p50 and may act as a co-activator to promote canonical NF κ B signaling [25]; thus, further studies are required to define the precise

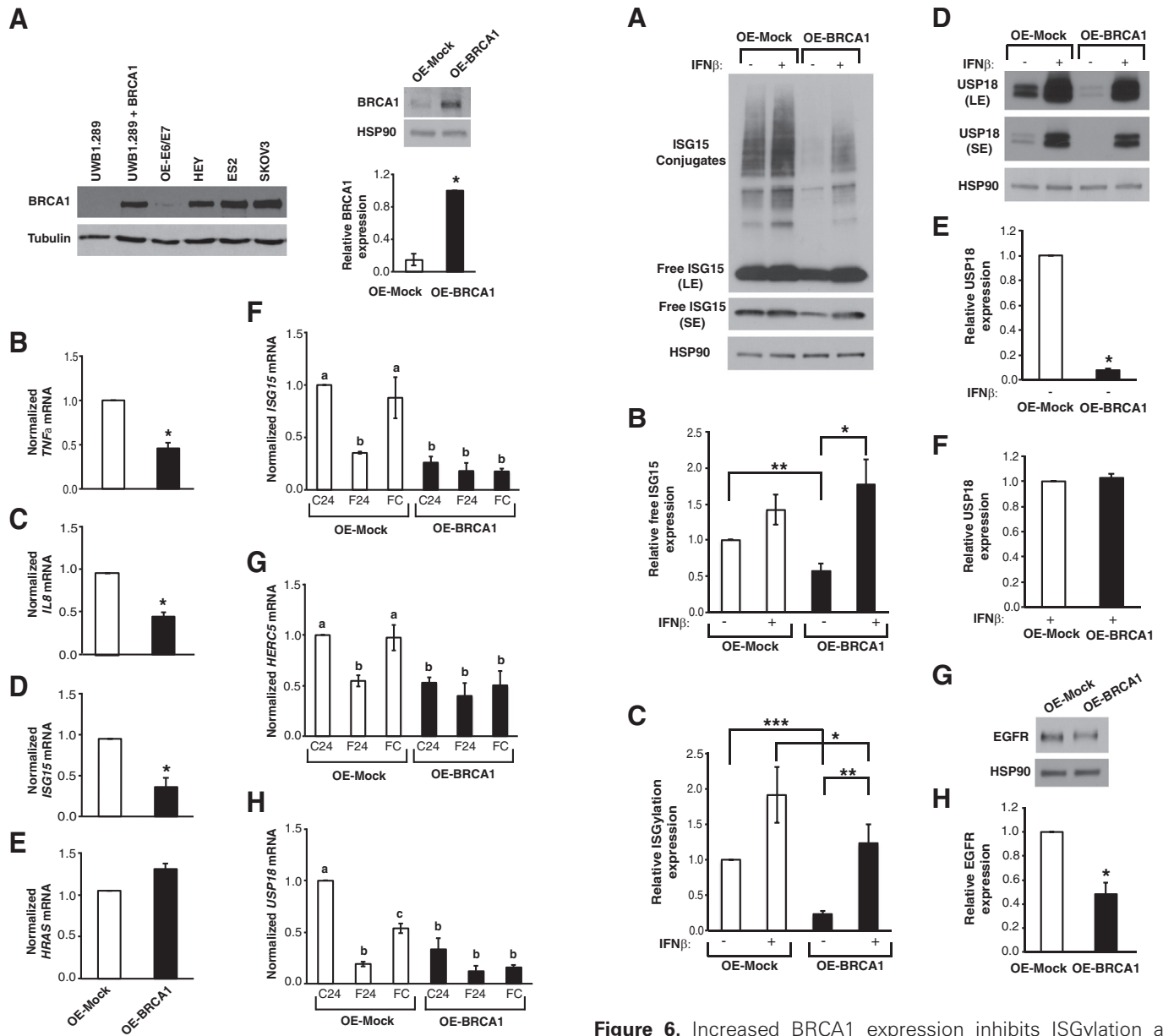
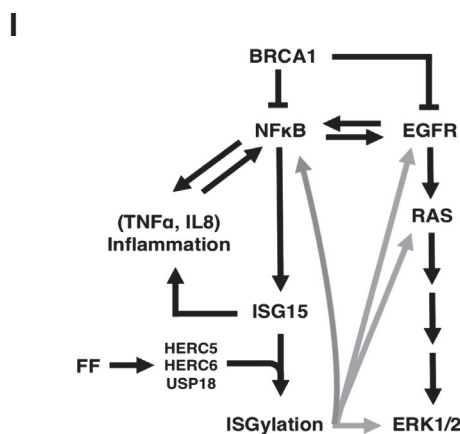
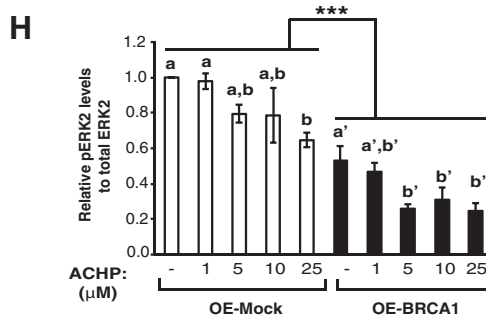
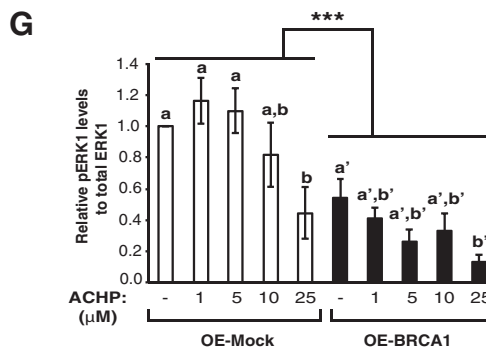
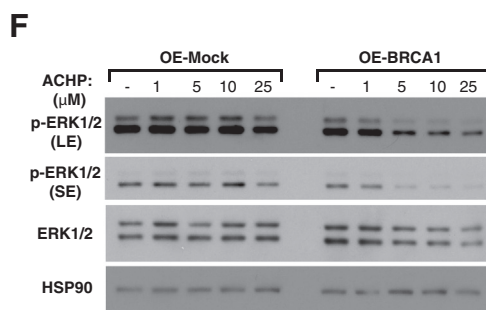
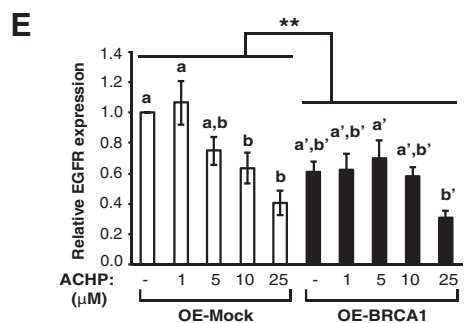
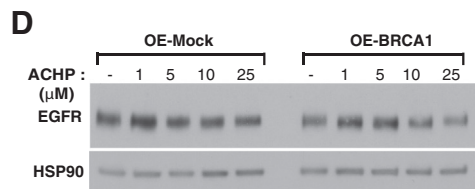
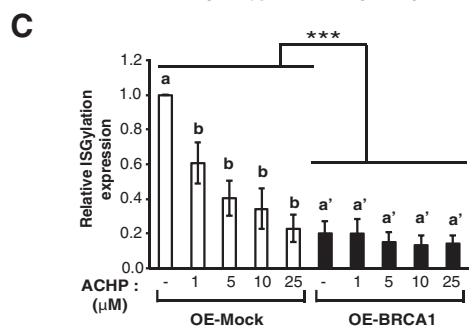
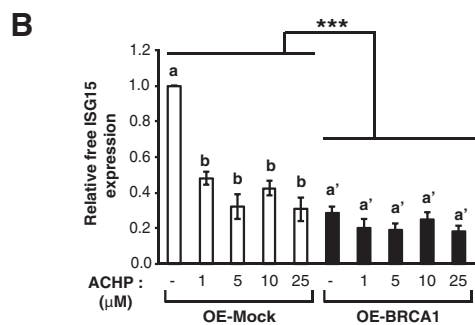
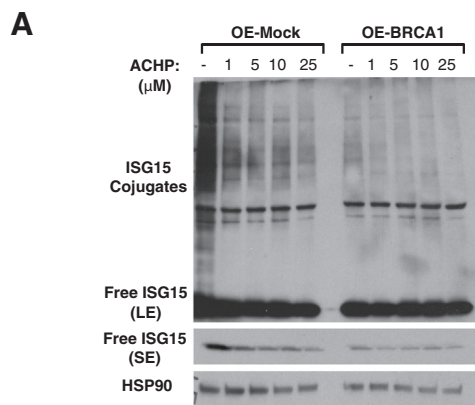


Figure 5. Increased BRCA1 expression inhibits expression of NF κ B target genes and alters the impact of FF exposure on expression of ISG15 and its interacting partners. (A) Left: Representative Western blot showing BRCA1 protein levels in OE-E6/E7 cells compared to ovarian cancer cell lines. UWB1.289 and UWB1.289+BRCA1 cells were used as a negative and positive control respectively. Right: Representative Western blot and comparison of BRCA1 levels in OE-Mock and OE-BRCA1 cells. Levels of HSP90 are shown as a loading control. Bars represent the mean \pm SEM of three independent experiments relative to levels measured in OE-BRCA1 cells. * P = .0075, one-sample t test. (B-E) Comparison of TNF α (B), IL8 (C), ISG15 (D), and HRAS (E) transcript levels in OE-Mock and OE-BRCA1 cells as determined by RT-qPCR. Bars represent the mean \pm SEM of three independent experiments relative to levels measured in OE-Mock cells. * P < .05, one-sample t test. (F-H) Comparison of ISG15 (F), HERC5 (G), and USP18 (H) transcript levels in OE-Mock and OE-BRCA1 at baseline (C24), after 24 hours of FF exposure (F24), and 24 hours after recovery from FF exposure (FC). Bars represent the mean \pm SEM of three (for HERC5 and USP18) or four (for ISG15) independent experiments relative to levels measured in OE-Mock cells at C24. Bars with different letters are statistically different from one another as determined by one-way ANOVA followed by SNK *post hoc* test.

Figure 6. Increased BRCA1 expression inhibits ISGylation and decreases ISG15, USP18, and EGFR protein levels. (A) Representative Western blot showing free and conjugated ISG15 levels in OE-Mock and OE-BRCA1 cells in the presence and absence of 24-hour treatment with 1000 U/ml IFN β . Levels of HSP90 are shown as a loading control. LE=long exposure; SE=short exposure. (B and C) Comparison of free ISG15 (B) and ISG15 conjugates (C) in OE-Mock and OE-BRCA1 cells in the presence or absence of IFN β treatment. Bars represent the mean \pm SEM of six independent experiments relative to levels measured in vehicle-treated OE-Mock cells. * P < .05; ** P < .01; *** P < .001, t test. (D) Representative Western blot showing USP18 levels in OE-Mock and OE-BRCA1 cells in the presence and absence of 24-hour treatment with 1000 U/ml IFN β . (E and F) Comparison of USP18 levels on OE-Mock and OE-BRCA1 cells in the absence (E) or presence (F) of IFN β treatment. Bars represent the mean \pm SEM of three independent experiments relative to levels measured in OE-Mock cells. Levels of USP18 following IFN β treatment were determined on short exposure blots. * P < .001, one-sample t test. (G) Representative Western blot showing levels of EGFR in OE-Mock and OE-BRCA1 cells. (H) Comparison of EGFR levels normalized to HSP90. Bars represent the mean \pm SEM of four independent experiments relative to levels measured in OE-Mock cells. * P < .02, one-sample t test.



mechanisms by which BRCA1 deficiency leads to increased NFκB signaling.

An inverse relationship between BRCA1 and EGFR has been identified in both breast and ovarian cancer [26,27]. This is consistent with our finding of increased EGFR target gene expression in *mtBRCA1* samples and a decrease in EGFR levels in OE-E6/E7 cells expressing increased wild-type BRCA1 levels. Inhibition of IKKα/β by ACHP reduced EGFR protein expression in both OE-Mock and OE-BRCA1 cells, indicating that EGFR signaling is downstream of NFκB. Since EGFR also activates NFκB signaling [28], this could lead to a positive feed-forward cycle between EGFR and NFκB in BRCA1-deficient cells.

Cross-talk between NFκB and EGFR signaling has been previously demonstrated by others. NFκB regulated KIAA1199/CEMIP was shown to increase EGFR signaling by reducing EGFR lysosome-dependent degradation in cervical and breast cancer cells [29]. Also, knockdown of IKKα and IKKβ suppressed EGFR signaling in head and neck cancer cells [30]. EGFR has also been shown to activate NFκB signaling either directly or indirectly through JAK/STAT signaling, leading to a positive feed-forward cycle between EGFR and NFκB [28,31–33]. Elevation of EGFR signaling pathways is involved in cell survival and growth. While activating mutations in downstream EGFR targets such as *RAS* and *ERK* are typically associated with low-grade serous ovarian carcinoma, EGFR amplification and overexpression in HGSOc have been reported [34].

Previous studies have indicated increased expression of type I interferon target genes in *BRCA1*- and *BRCA2*-deficient cells relative to controls in multiple cell types, including breast and HGSOc cells [21,35]; however, this increase did not fully emerge in our nonmalignant primary FTE cell cultures until after FF exposure. Increased *ISG15* transcripts were identified in *mtBRCA1* compared to control samples at both baseline and after recovery from FF exposure. *ISG15* expression is increased in many epithelial cancers [36–38] and contributes to RAS-induced oncogenic transformation of breast epithelial cells [39].

ISG15 functions in protein modification and as a mature free protein. While free *ISG15* is found intracellularly, it is also secreted and acts upon lymphocytes to induce release of IFNγ and possibly other cytokines [40]. Secreted *ISG15* was shown to suppress tumor growth, increase natural killer cell tumor infiltration, and enhance cell surface MHC class I expression in breast tumors [41]. Thus, free

ISG15 may have a different impact on cancer progression than increased ISGylation. BRCA1 expression in OE-E6/E7 cells decreased both free *ISG15* and ISGylated protein levels. This suggests that BRCA1 deficiency directly results in increased *ISG15* expression and demonstrates a functional impact of the altered transcript levels. Several *ISG15* E3 ligases have been identified that determine substrate specificity for ISGylation. Among these, *HERC5*, which was upregulated in OE-Mock versus OE-BRCA1 cells and in *mtBRCA1* versus control samples after FF recovery, is the most common and has a wide range of target proteins [42].

ISGylation has been implicated in cancer development and progression. Desai et al. [43] demonstrated that ISGylation disrupts F-actin architecture and formation of focal adhesions, and promotes migration in breast cancer cells. Induction of ISGylation in mice exacerbates intestinal inflammation, increases ROS, and promotes generation of colitis-associated colon cancer [44]. *ISG15* protein expression is increased in relapsed HGSOcs compared to primary tumors [45]. As well, 20% of ovarian cancer cases express an “interferon-related” gene signature that includes *ISG15* [46]. Over 150 ISGylated proteins have been identified [47]; however, the impact of ISGylation on function has only been investigated for a limited number of targets.

ISG15 expression is upregulated by TNFα [48] and has dual effects on NFκB signaling [49,50]. We demonstrated that blocking NFκB activation decreased *ISG15* expression and overall ISGylation in OE-Mock cells to levels measured in OE-BRCA1 cells, indicating that BRCA1 deficiency increases *ISG15* levels through increased NFκB signaling. ERK1 has been identified as an ISGylation target [51], and we found increased ERK1/2 activation associated with decreased BRCA1 expression. Further studies are required to determine if ISGylation is involved in the impact of BRCA1 deficiency on ERK1/2 activation as inhibitors to this protein modification pathway are currently unavailable.

ISGylation is reversible through the deconjugating activity of *USP18* [52,53]. *USP18* transcripts were not increased in *mtBRCA1* samples at baseline and emerged as significantly elevated only after FF exposure, when *HERC5* transcripts were also elevated. Increased BRCA1 levels in OE-E6/E7 cells decreased *ISG15*, *HERC5*, and *USP18* transcripts; however, unlike the primary cultures, this impact on *HERC5* and *USP18* was detected at baseline. FF exposure

Figure 7. Increased NFκB activity in BRCA1-deficient cells leads to increased *ISG15* and may contribute to increased EGFR signaling. (A) Representative Western blot showing levels of free and conjugated *ISG15* in OE-Mock and OE-BRCA1 cells following inhibition of NFκB signaling by increasing doses of ACHP for 48 hours. Levels of HSP90 are shown as a loading control. LE=long exposure; SE=short exposure. (B and C) Comparison of free (B) and conjugated *ISG15* (C) levels normalized to HSP90. Bars represent the mean ± SEM of four independent experiments relative to levels measured in vehicle-treated OE-Mock cells. Two-way ANOVA indicated a significant effect of BRCA1 expression ($P<.0001$), ACHP treatment ($P<.0001$), and interaction ($P<.0001$, free; $P<.002$, conjugated). The effect of ACHP treatment was analyzed separately for OE-Mock and for OE-BRCA1 cells by one-way ANOVA followed by SNK *post hoc* test. Bars with different letters within each cell subtype are statistically different from one another. (D) Representative Western blot showing levels of EGFR in OE-Mock and OE-BRCA1 cells following ACHP treatment. (E) Comparison of EGFR levels normalized to HSP90 in four independent experiments. Levels are relative to vehicle-treated OE-Mock cells. Two-way ANOVA indicated a significant effect of BRCA1 expression ($P<.002$) and ACHP treatment ($P<.0001$), but not interaction. The effect of ACHP treatment was analyzed separately for OE-Mock and for OE-BRCA1 cells by one-way ANOVA followed by SNK *post hoc* test. (F) Representative Western blot showing levels of pERK1/2 in OE-Mock and OE-BRCA1 cells following ACHP treatment. (G and H) Comparison of pERK1 (G) and pERK2 (H) levels normalized to total ERK1 or total ERK2 levels in four independent experiments. Levels are relative to vehicle-treated OE-Mock cells. Two-way ANOVA indicated a significant effect of BRCA1 expression ($P<.0001$) and ACHP treatment ($P<.002$, pERK1; $P<.0002$, pERK2), but no interaction. The effect of ACHP treatment was analyzed separately for OE-Mock and for OE-BRCA1 cells by one-way ANOVA followed by SNK *post hoc* test. (I) Schematic model for the impact of BRCA1 expression on suppression of inflammatory signaling and ISGylation. ISGylation targets multiple proteins including the EGFR and several members of the downstream MAPK signaling cascade.

transiently suppressed transcript levels of all three genes in OE-Mock cells to levels similar to those measured in OE-BRCA1 cells, which were unaffected by FF. The variation in overall gene expression between patients could have prevented the interferon gene expression signal reaching statistical significance at baseline in the primary cultures. Alternatively, expression of *ISG15* interacting partners may vary at baseline but has a concerted response to FF exposure and recovery. It is interesting to note that increased USP18 expression did not prevent the increase in ISGylated protein levels. However, USP18 has independent direct effects on tumor growth and survival and enhances EGFR signaling by decreasing miR-7 expression, which targets EGFR [54]. Thus, USP18 may contribute to increased EGFR signaling.

While we had expected the combination of FF and *BRCA1* mutation would globally increase proinflammatory signaling, FF exposure appeared to transiently suppress several inflammatory genes in mt*BRCA1* cells to the level of controls. Steroid hormones, which are found at high levels in FF, have been shown to decrease NFκB signaling [55–57]. As well, androgens decrease expression of *ISG15* and its interacting partners [38]. Exposure to these hormones in FF may transiently reduce the baseline elevation in inflammatory signaling in mt*BRCA1* cells to the levels of controls by eliminating their relative increase in NFκB activity.

As summarized in Figure 7I, the present study highlights an increase in ISG15 and ISGylation resulting from *BRCA1* deficiency and FF exposure. This increase appears to be mediated through increased NFκB signaling due to low levels of functional *BRCA1*. ISGylation targets multiple proteins, including proteins involved in EGFR and MAPK-ERK1/2 signaling, and has been linked to cancer initiation through increased inflammatory signaling [44]. Although not tested, increased ISGylation of EGFR-MAPK-ERK1/2 cascade members might contribute to increased pERK1/2 levels associated with decreased *BRCA1*. It remains to be determined if blocking ISGylation in *BRCA1*-deficient FTE results in decreased proinflammatory and EGFR signaling and whether this might mitigate the risk for malignant transformation.

Supplementary data to this article can be found online at <https://doi.org/10.1016/j.neo.2018.05.005>.

Acknowledgements

We thank Natalie Stickle for help with data analyses.

References

- [1] Crum CP, Drapkin R, Miron A, Ince TA, Muto M, Kindelberger DW, and Lee Y (2007). The distal fallopian tube: a new model for pelvic serous carcinogenesis. *Curr Opin Obstet Gynecol* **19**, 3–9.
- [2] Chen S and Parmigiani G (2007). Meta-analysis of *BRCA1* and *BRCA2* penetrance. *J Clin Oncol* **25**, 1329–1333.
- [3] King MC, Marks JH, and Mandell JB (2003). Breast and ovarian cancer risks due to inherited mutations in *BRCA1* and *BRCA2*. *Science* **302**, 643–646.
- [4] Mavaddat N, Peock S, Frost D, Ellis S, Platte R, Fineberg E, Evans DG, Izatt L, Eeles RA, and Adlard J, et al (2013). Cancer risks for *BRCA1* and *BRCA2* mutation carriers: results from prospective analysis of EMBRACE. *J Natl Cancer Inst* **105**, 812–822.
- [5] Boyd J, Sonoda Y, Federici MG, Bogomolny F, Rhei E, Maresco DL, Saigo PE, Almadrone LA, Barakat RR, and Brown CL, et al (2000). Clinicopathologic features of *BRCA*-linked and sporadic ovarian cancer. *JAMA* **283**, 2260–2265.
- [6] Havrilesky LJ, Moorman PG, Lowery WJ, Gierisch JM, Coeytaux RR, Urrutia RP, Dinan M, McBroom AJ, Hasselblad V, and Sanders GD, et al (2013). Oral contraceptive pills as primary prevention for ovarian cancer: a systematic review and meta-analysis. *Obstet Gynecol* **122**, 139–147.
- [7] Tung KH, Wilkens LR, AH Wu, McDuffie K, Nomura AM, Kolonel LN, Terada KY, and Goodman MT (2005). Effect of anovulation factors on pre- and postmenopausal ovarian cancer risk: revisiting the incessant ovulation hypothesis. *Am J Epidemiol* **161**, 321–329.
- [8] McGuire V, Felberg A, Mills M, Ostrow KL, DiCioccio R, John EM, West DW, and Whittemore AS (2004). Relation of contraceptive and reproductive history to ovarian cancer risk in carriers and noncarriers of *BRCA1* gene mutations. *Am J Epidemiol* **160**, 613–618.
- [9] McLaughlin JR, Risch HA, Lubinski J, Moller P, Ghadirian P, Lynch H, Karlan B, Fishman D, Rosen B, and Neuhausen SL, et al (2007). Reproductive risk factors for ovarian cancer in carriers of *BRCA1* or *BRCA2* mutations: a case-control study. *Lancet Oncol* **8**, 26–34.
- [10] Buscher U, Chen FC, Kentenich H, and Schmiady H (1999). Cytokines in the follicular fluid of stimulated and non-stimulated human ovaries; is ovulation a suppressed inflammatory reaction? *Hum Reprod* **14**, 162–166.
- [11] Fleming JS, Beaugie CR, Haviv I, Chenevix-Trench G, and Tan OL (2006). Incessant ovulation, inflammation and epithelial ovarian carcinogenesis: revisiting old hypotheses. *Mol Cell Endocrinol* **247**, 4–21.
- [12] Tone AA, Begley H, Sharma M, Murphy J, Rosen B, Brown TJ, and Shaw PA (2008). Gene expression profiles of luteal phase fallopian tube epithelium from *BRCA* mutation carriers resemble high-grade serous carcinoma. *Clin Cancer Res* **14**, 4067–4078.
- [13] Tone AA, Virtanen C, Shaw P, and Brown TJ (2012). Prolonged postovulatory proinflammatory signaling in the fallopian tube epithelium may be mediated through a *BRCA1/DAB2* axis. *Clin Cancer Res* **18**, 4334–4344.
- [14] Fotheringham S, Levanon K, and Drapkin R (2011). Ex vivo culture of primary human fallopian tube epithelial cells. *J Vis Exp* **51**, 2728. doi:10.3791/2728.
- [15] Lee YL, Lee KF, JS Xu, Wang YL, Tsao SW, and Yeung WS (2001). Establishment and characterization of an immortalized human oviductal cell line. *Mol Reprod Dev* **59**, 400–409.
- [16] Lau A, Kollara A, St John E, Tone AA, Virtanen C, Greenblatt EM, King WA, and Brown TJ (2014). Altered expression of inflammation-associated genes in oviductal cells following follicular fluid exposure: implications for ovarian carcinogenesis. *Exp Biol Med (Maywood)* **239**, 24–32.
- [17] Bahar-Shany K, Brand H, Sapoznik S, Jacob-Hirsch J, Yung Y, Korach J, Perri T, Cohen Y, Hourvitz A, and Levanon K (2014). Exposure of fallopian tube epithelium to follicular fluid mimics carcinogenic changes in precursor lesions of serous papillary carcinoma. *Gynecol Oncol* **132**, 322–327.
- [18] Johnson WE, Li C, and Rabinovic A (2007). Adjusting batch effects in microarray expression data using empirical Bayes methods. *Biostatistics* **8**, 118–127.
- [19] Shannon P, Markiel A, Ozier O, Baliga NS, Wang JT, Ramage D, Amin N, Schwikowski B, and Ideker T (2003). Cytoscape: a software environment for integrated models of biomolecular interaction networks. *Genome Res* **13**, 2498–2504.
- [20] Loeb KR and Haas AL (1992). The interferon-inducible 15-kDa ubiquitin homolog conjugates to intracellular proteins. *J Biol Chem* **267**, 7806–7813.
- [21] H Xu, Xian J, Vire E, McKinney S, Wei V, Wong J, Tong R, Kouzarides T, Caldas C, and Aparicio S (2014). Up-regulation of the interferon-related genes in *BRCA2* knockout epithelial cells. *J Pathol* **234**, 386–397.
- [22] Ezell SA, Polytaichou C, Hatziaepostolou M, Guo A, Sanidas I, Bihani T, Comb MJ, Sourvinos G, and Tsihchlis PN (2012). The protein kinase Akt1 regulates the interferon response through phosphorylation of the transcriptional repressor EMSY. *Proc Natl Acad Sci U S A* **109**, E613–621.
- [23] Hoesel B and Schmid JA (2013). The complexity of NF-κB signaling in inflammation and cancer. *Mol Cancer* **12**(86), 1–15.
- [24] Sau A, Lau R, Cabrita MA, Nolan E, Crooks PA, Visvader JE, and Pratt MA (2016). Persistent Activation of NF-κappaB in *BRCA1*-Deficient Mammary Progenitors Drives Aberrant Proliferation and Accumulation of DNA Damage. *Cell Stem Cell* **19**, 52–65.
- [25] Benezra M, Chevallier N, Morrison DJ, MacLachlan TK, El-Deiry WS, and Licht JD (2003). *BRCA1* augments transcription by the NF-κappaB transcription factor by binding to the Rel domain of the p65/RelA subunit. *J Biol Chem* **278**, 26333–26341.
- [26] LN Burga H Hu, Juvekar A, Tung NM, Troyan SL, Hofstatter EW, and Wulf GM (2011). Loss of *BRCA1* leads to an increase in epidermal growth factor receptor expression in mammary epithelial cells, and epidermal growth factor receptor inhibition prevents estrogen receptor-negative cancers in *BRCA1*-mutant mice. *Breast Cancer Res* **13**, R30.
- [27] Li D, Bi FF, Cao JM, Cao C, Li CY, and Yang Q (2013). Effect of *BRCA1* on epidermal growth factor receptor in ovarian cancer. *J Exp Clin Cancer Res* **32**, 102. doi:10.1186/1756-9966-32-102 6 pp.

- [28] De S, Dermawan JK, and Stark GR (2014). EGF receptor uses SOS1 to drive constitutive activation of NF-kappaB in cancer cells. *Proc Natl Acad Sci U S A* **111**, 11721–11726.
- [29] Shostak K, Zhang X, Hubert P, Goktuna SI, Jiang Z, Klevernic I, Hildebrand J, Roncarati P, Henny B, and Ladang A, et al (2014). NF-kappaB-induced KIAA1199 promotes survival through EGFR signalling. *Nat Commun* **5**, 5232. doi:10.1038/ncomms6232 19 pp.
- [30] Nottingham LK, Yan CH, Yang X, Si H, Coupar J, Bian Y, TF Cheng C, Allen P, and Arun D Gius, et al (2014). Aberrant IKKalpha and IKKbeta cooperatively activate NF-kappaB and induce EGFR/AP1 signaling to promote survival and migration of head and neck cancer. *Oncogene* **33**, 1135–1147.
- [31] Biswas DK, Cruz AP, Gansberger E, and Pardee AB (2000). Epidermal growth factor-induced nuclear factor kappa B activation: A major pathway of cell-cycle progression in estrogen-receptor negative breast cancer cells. *Proc Natl Acad Sci U S A* **97**, 8542–8547.
- [32] Le Page C, Koumakpayi IH, Lessard L, Mes-Masson AM, and Saad F (2005). EGFR and Her-2 regulate the constitutive activation of NF-kappaB in PC-3 prostate cancer cells. *Prostate* **65**, 130–140.
- [33] Jiang T, Grabiner B, Zhu Y, Jiang C, Li H, You Y, Lang J, Hung MC, and Lin X (2011). CARMA3 is crucial for EGFR-Induced activation of NF-kappaB and tumor progression. *Cancer Res* **71**, 2183–2192.
- [34] Lassus H, Sihto H, Leminen A, Joensuu H, Isola J, Nupponen NN, and Butzow R (2006). Gene amplification, mutation, and protein expression of EGFR and mutations of ERBB2 in serous ovarian carcinoma. *J Mol Med (Berl)* **84**, 671–681.
- [35] Jazaeri AA, Yee CJ, Sotiriou C, Brantley KR, Boyd J, and Liu ET (2002). Gene expression profiles of BRCA1-linked, BRCA2-linked, and sporadic ovarian cancers. *J Natl Cancer Inst* **94**, 990–1000.
- [36] Chi LM, Lee CW, Chang KP, Hao SP, HM Lee Y, Liang C, Hsueh CJ Yu, Lee IN, and Chang YJ, et al (2009). Enhanced interferon signaling pathway in oral cancer revealed by quantitative proteome analysis of microdissected specimens using 16O/18O labeling and integrated two-dimensional LC-ESI-MALDI tandem MS. *Mol Cell Proteomics* **8**, 1453–1474.
- [37] Andersen JB, Aaboe M, Borden EC, Goloubeva OG, Hassel BA, and Orntoft TF (2006). Stage-associated overexpression of the ubiquitin-like protein, ISG15, in bladder cancer. *Br J Cancer* **94**, 1465–1471.
- [38] Kiessling A, Hogrefe C, Erb S, Bobach C, Fuessel S, Wessjohann L, and Seliger B (2009). Expression, regulation and function of the ISGylation system in prostate cancer. *Oncogene* **28**, 2606–2620.
- [39] Tsai YC, Pestka S, Wang LH, Runnels LW, Wan S, Lyu YL, and Liu LF (2011). Interferon-beta signaling contributes to Ras transformation. *PLoS One* **6**e24291.
- [40] Bogunovic D, Boisson-Dupuis S, and Casanova JL (2013). ISG15: leading a double life as a secreted molecule. *Exp Mol Med* **45**, e18.
- [41] Burks J, Reed RE, and Desai SD (2015). Free ISG15 triggers an antitumor immune response against breast cancer: a new perspective. *Oncotarget* **6**, 7221–7231.
- [42] Dastur A, Beaudenon S, Kelley M, Krug RM, and Huijbregtse JM (2006). Herc5, an interferon-induced HECT E3 enzyme, is required for conjugation of ISG15 in human cells. *J Biol Chem* **281**, 4334–4338.
- [43] Desai SD, Reed RE, Burks J, Wood LM, Pullikuth AK, Haas AL, Liu LF, Breslin JW, Meiners S, and Sankar S (2012). ISG15 disrupts cytoskeletal architecture and promotes motility in human breast cancer cells. *Exp Biol Med* **237**, 38–49.
- [44] Fan JB, Miyauchi-Ishida S, Arimoto K, Liu D, Yan M, Liu CW, Gyorffy B, and Zhang DE (2015). Type I IFN induces protein ISGylation to enhance cytokine expression and augments colonic inflammation. *Proc Natl Acad Sci U S A* **112**, 14313–14318.
- [45] Darb-Esfahani S, Sinn BV, Rudl M, Sehouli J, Braicu I, Dietel M, and Denkert C (2014). Interferon-stimulated gene, 15 kDa (ISG15) in ovarian high-grade serous carcinoma: prognostic impact and link to NF-kappaB pathway. *Int J Gynecol Pathol* **33**, 16–22.
- [46] Einav U, Tabach Y, Getz G, Yitzhaky A, Ozbek U, Amariglio N, Izraeli S, Rechavi G, and Domany E (2005). Gene expression analysis reveals a strong signature of an interferon-induced pathway in childhood lymphoblastic leukemia as well as in breast and ovarian cancer. *Oncogene* **24**, 6367–6375.
- [47] Zhao C, Denison C, Huijbregtse JM, Gygi S, and Krug RM (2005). Human ISG15 conjugation targets both IFN-induced and constitutively expressed proteins functioning in diverse cellular pathways. *Proc Natl Acad Sci U S A* **102**, 10200–10205.
- [48] Chairatvit K, Wongnoppavich A, and Choonate S (2012). Up-regulation of interferon-stimulated gene15 and its conjugates by tumor necrosis factor-alpha via type I interferon-dependent and -independent pathways. *Mol Cell Biochem* **368**, 195–201.
- [49] Minakawa M, Sone T, Takeuchi T, and Yokosawa H (2008). Regulation of the nuclear factor (NF)-kappaB pathway by ISGylation. *Biol Pharm Bull* **31**, 2223–2227.
- [50] Takeuchi T, Kobayashi T, Tamura S, and Yokosawa H (2006). Negative regulation of protein phosphatase 2Cbeta by ISG15 conjugation. *FEBS Lett* **580**, 4521–4526.
- [51] Malakhov MP, Kim KI, Malakhova OA, Jacobs BS, Borden EC, and Zhang DE (2003). High-throughput immunoblotting. Ubiquitin-like protein ISG15 modifies key regulators of signal transduction. *J Biol Chem* **278**, 16608–16613.
- [52] Liu LQ, Ilaria Jr R, Kingsley PD, Iwama A, van Etten RA, and Palis J (1999). DE Zhang. A novel ubiquitin-specific protease, UBP43, cloned from leukemia fusion protein AML1-ETO-expressing mice, functions in hematopoietic cell differentiation. *Mol Cell Biol* **19**, 3029–3038.
- [53] Mustachio LM, Lu Y, Kawakami M, Roszik J, Freemantle SJ, Liu X, and Dmitrovsky E (2018). Evidence for the ISG15-Specific Deubiquitinase USP18 as an Antineoplastic Target. *Cancer Res* **78**, 587–592.
- [54] Honke N, Shaabani N, Zhang DE, Hardt C, and Lang KS (2016). Multiple functions of USP18. *Cell Death Dis* **7**e2444.
- [55] He YH, Zhang HN, Zhang GP, Hou N, Xiao Q, Huang Y, Wu JH, Luo MS, Zhang GS, and Yi Q, et al (2011). A physiological concentration of glucocorticoid inhibits the pro-inflammatory cytokine-induced proliferation of adult rat cardiac fibroblasts: roles of extracellular signal-regulated kinase 1/2 and nuclear factor-kappaB. *Clin Exp Pharmacol Physiol* **38**, 739–746.
- [56] Lei B, Mace B, Dawson HN, Warner DS, Laskowitz DT, and James ML (2014). Anti-inflammatory effects of progesterone in lipopolysaccharide-stimulated BV-2 microglia. *PLoS One* **9**e103969.
- [57] Xing D, Oparil S, Yu H, Gong K, Feng W, Black J, Chen YF, and Nozell S (2012). Estrogen modulates NFkappaB signaling by enhancing IkappaBalpha levels and blocking p65 binding at the promoters of inflammatory genes via estrogen receptor-beta. *PLoS One* **7**e36890.